ADVANCED FUNCTIONAL MATERIALS
www.afm-journal.de

Hydrogen-Terminated Si Nanowires as Label-Free Colorimetric Sensors in the Ultrasensitive and Highly Selective Detection of Fluoride Anions in Pure Water Phase

*Hui Wang, Pei-Hong Fan, Bin Tong, Yu-Ping Dong, Xue-Mei Ou, Fan Li, and Xiao-Hong Zhang**

The detection of anions in pure water phase with colorimetric sensor is a long standing challenge. As one of the most important anions, F^- is associated with nerve gases and the refinement of uranium for nuclear weapons. However, limited by its anions nature, few of the reported colorimetric sensors can successfully applied to detect F^{-1} in pure water phase. This work designs a colorimetric sensor for F^{-1} pure water phase detection by taking the advantages of the strong specific binding between F and Si, as well as the color-changing property of H-terminated Si nanowires (SiNWs). The sensor demonstrates ultra-sensitivity, high selectivity, and good stability. The results reveal particular interest for the development of new type aqueous phase anions sensors with SiNWs.

1. Introduction

The use of nanostructures in the development of sensors and receptors for ultrasensitive and highly selective detection is currently of great interest because nanostructures possess optical, electronic, and structural properties that are unavailable in bulk materials.[1–5] Colorimetric sensors developed using nanostructures such as Au nanoparticles (NPs) can transform detected events into color changes that can be conveniently perceived by the naked eye. Thus, nanostructures can be applied in field analysis and point-of-care diagnosis.[6–8] The use of nanostructures, such as Au, Ag, semiconductor, and metal oxide NPs, as well as carbon nanotube and graphene oxide, as alternative colorimetric sensors to traditional organic chemical sensors has been intensively studied, especially with regard to advanced aqueous phase detection.[9–14] These colorimetric sensors have been applied in the detection of living cells,[9] DNA sequences,[10] proteins,[11] and biologically important cations.[12,13] These sensors also demonstrate high sensitivity (e.g., zeptomole sensitivity[14] and selectivity (e.g., selectivity factor of 100 000:1[15] that are difficult to achieve using conventional methods.

Aqueous phase detection is important because it encompasses most of the biological and environmental detections, including the detection of drinking water. Although colorimetric sensors have demonstrated more advantages in aqueous detection than traditional organic chemical sensors, the development of such sensors using nanostructures remains a challenge because their surfaces must be tailored to improve their dispersibility, selectivity, and stability.[5,16–25] The most commonly used nanostructures, such as carbon nanotube and graphene oxide, have hydrophobic surfaces, which should therefore be modified to improve their dispersibility in water.[16,17] Similarly, metal and semiconductor NPs require surface modification to achieve practical stability.[18–20] Moreover, the surfaces of these nanostructures generally require labeling by affinity ligands, such as antibodies and aptamers, in order to interact specifically with the detection target to achieve high sensibility and selectivity because they are not specifically bound to analytes.[21–25] However, affinity ligands not only require complicated and time-consuming multistep synthetic pathways and purification but also possess serious intrinsic disadvantages; they are easily denatured and digested by proteases. Therefore, the development of an aqueous phase detection strategy with simplified surface tailoring is worth pursuing.

In this work, we propose a new aqueous phase detection strategy that can significantly simplify surface decoration by designing sensors with stable 1D nanostructures which are specifically bound to analytes. We demonstrate that H-terminated Si nanowires (H-SiNWs) can be used as stable colorimetric sensor for F^{-1} detection in pure water phase with ultrasensitivity, high selectivity, and good stability.

Dr. H. Wang, X. Ou, F. Li, Prof. X. Zhang
Nano-organic Photoelectronic Laboratory
and Key Laboratory of Photochemical Conversion
and Optoelectronic Materials
Technical Institute of Physics and Chemistry
Chinese Academy of Sciences
Beijing 100190, P.R. China
E-mail: xhzhang@mail.ipc.ac.cn
P. Fan, B. Tong, Prof. Y. Dong
College of Materials Science and Engineering
Beijing Institute of Technology
5 South Zhongguancun Street, Beijing 100081, P.R. China
Prof. X. Zhang
Functional Nano and Soft Materials Laboratory (FUNSOM)
Jiangsu Key Laboratory for Carbon-Based Functional Materials
and Devices and Collaborative Innovation Center of Suzhou
Nano Science and Technology
Soochow University
Suzhou, Jiangsu 215123, P.R. China

DOI: 10.1002/adfm.201401632

2. Results and Discussion

The detection of anions in the aqueous phase is a topic that has attracted the interest of chemists and biologists because of the important roles played by anions in living organisms. But as anions are generally larger than cations such as metal ions, they are much more easy to be solvated than cations and thus then hard to be selectively detected by sensor. Moreover, as solvation will become stronger in high polar solvent such as water; therefore, although many approaches had been developed to detect anions in organic solution; however, few of them can be successfully applied to pure water phase.[26–29]

F^{-1} is one of the most important anions because it is associated with nerve gases, the refinement of uranium for nuclear weapons, and the drinking water supplies for dental care. The fluoride levels recommended by the US Health and Human Services range from 1.2 to 0.7 ppm.[30] Numerous colorimetric sensors have been developed to detect F^- ions using the Lewis acidic interaction, H-bond coordination, and fluoride-triggered Si–O bond cleavage mechanism.[26,28,31] However, most of these sensors either work only in organic solutions or require organic solutions for application in the aqueous phase because of their hydrophobic chromophores.[26–31]

H-SiNWs can be considered as aqueous phase colorimetric sensors for F^- because Si has a specific binding to F, and their bond dissociation energies can be as high as 540 kJ mol^{-1}. Consequently, the strong interaction between H-SiNWs and F^- can cause aggregation of SiNWs in solution; which further induce an apparent color change since H-SiNWs have appropriate light scattering and absorption properties. The color change can be attributed to SiNW's nature. First, SiNWs undergo intrinsic polarization anisotropy in absorption and emission because its 1D morphology confines electron movement.[32] Second, the quantization effects induced as a result of the small diameter of SiNWs increase carrier binding energies and result in optical properties that differ from those of thin films and bulk materials.[33] Third, random SiNWs have significant diffuse reflectivity induced by multiple scattering and can thus scatter incident light strongly.[34] Fourth, Si has a high refractive index (refractive index $n = 3.5$). SiNWs with diameters in the order of the wavelength of visible light significantly enhance the resonant field of incident light.[35] The calculated absorption and emission efficiencies of SiNWs with a diameter of 200 nm under an incident light wavelength of 350 nm may be 901% and 449%, respectively.[35] These interactions between scattering and absorption properties result in SiNWs with appearance of either yellow or brown, which is dramatically different from the black appearance of the Si wafer. The color change property was utilized in the current work to design the colorimetric sensor.

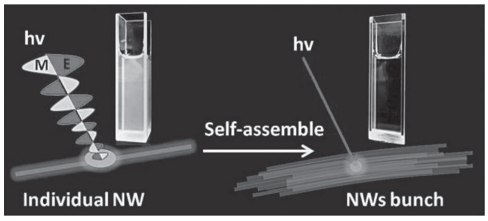

Figure 1. Proposed schedule for the use of SiNWs as colorimetric sensors based on their structural properties. M and E represent the magnetic and electric fields, respectively.

A proposed schedule for the use of SiNWs as colorimetric sensors in F^{-1} detection is presented in **Figure 1**. The H-SiNW suspension in the aqueous phase appears yellow; the color of the system fades when F^- modifies the assembly process and individual SiNWs are assembled into clusters. The resultant color change process can be utilized for F^- detection.

The detection process and the proposed F^{-1} anion detection mechanism using SiNWs as colorimetric sensors are shown in **Figure 2**. The SiNWs were first prepared using the vapor–liquid–solid method with Sn as a catalyst.[36] The SiNWs were then treated with hydrofluoric acid (HF) solution (5%) to remove the SiO_2 layer coating the surface and to obtain H-SiNWs. The results were established with energy dispersive X-ray spectroscopy (EDX). The H-SiNWs were dispersed in deionized water after being washed with deionized water to remove the residual HF (Figure 2A) before they were dispersed in cetyltrimethylammonium bromide (CTAB, 0.9×10^{-3} mol L^{-1}, Figure 2B). Then potassium fluoride (KF, 2×10^{-2} mol L^{-1}, Figure 2C) were used to titrate the SiNW suspension for F^- detection.

Although the yellow color of the H-SiNW stock suspension remains stable for years when sealed in a flask, the color quickly fades from yellow to clear after F^- is introduced. The

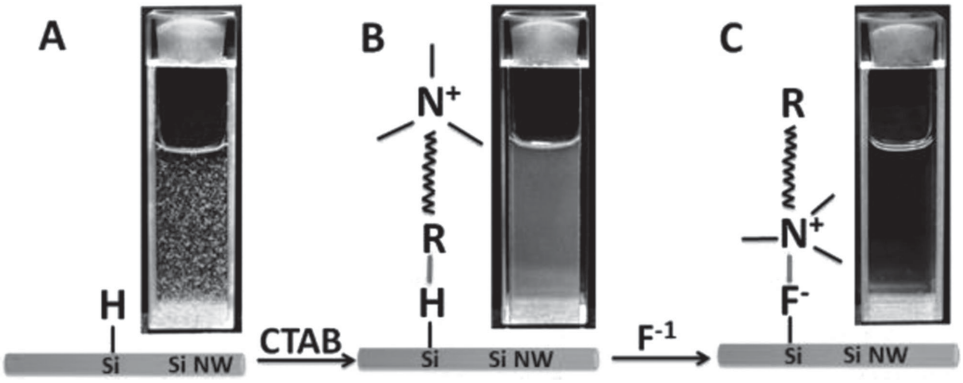

Figure 2. SiNW color and the proposed surface microstructure. A) H-SiNWs suspended in water. B) H-SiNWs dispersed in CTAB solution. C) Transparent system resulting from the presence of F^-.

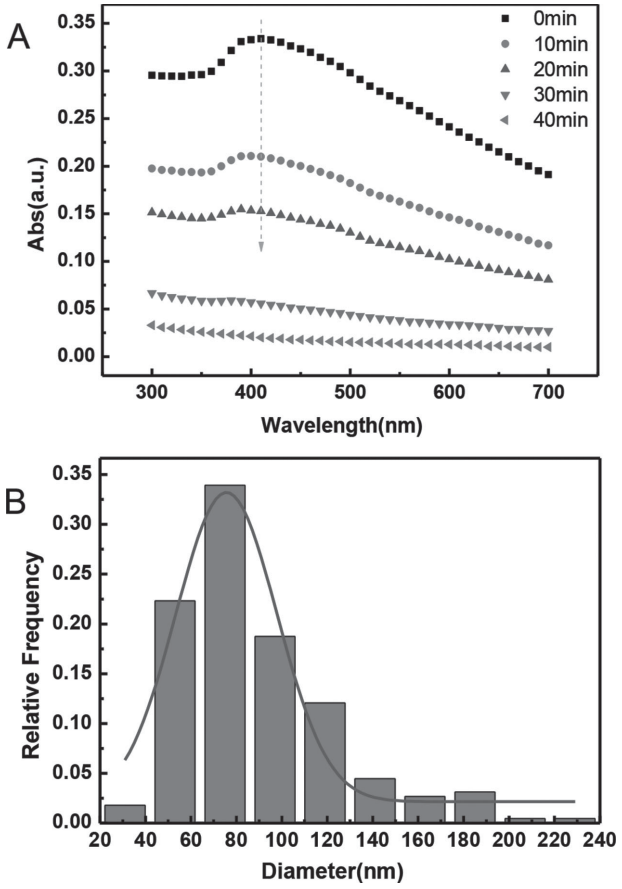

Figure 3. A) UV–vis spectroscopy of the SiNWs–CTAB–KF system. The CTAB and KF concentrations are 0.9×10^{-3} and 2×10^{-2} mol L^{-1}, respectively. B) Diameter distribution of SiNWs in the experiment based on 400 SEM image samples.

color variation may be attributed to the aggregation of SiNWs. SiNWs may aggregate into coils in deionized water because their H-terminated surfaces are strongly hydrophobic.[37] Consequently, SiNWs remain as a small cluster when suspended in water even if they are vigorously agitated or treated with ultrasonic (Figure 2A). The long-time stability in color and strongly hydrophobic surface of SiNWs also indicate the removal of residual surface ions, such as F^-. Even though few F^- (under the detection limit of EDX) are left, the concentration is so low that they may not significantly affect the aggregation of SiNWs and the sensing of adding F^-.

Studies suggest that when CTAB enters the system, its hydrophobic aliphatic chain attaches to the H-SiNW surface, and CTAB discards its ammonium ions in the water. The H-SiNW coils become untied, thus inducing the dispersion of SiNWs in the water (Figure 2B). The F^- anion introduced to the system may replace the aliphatic CTAB chain on the SiNW surface because the bond energy of the F–Si bond is strong. The negatively charged F^- anions then attract the positively charged ammonium ions to form the SiNW–F^-–N^+–R structure (Figure 2C). This result indicates the exposure of the hydrophobic aliphatic chain of CTAB in the water. Consequently, the SiNW–F^-–N^+–R structure self-assembles into a cluster in the water via the aliphatic chain. The SiNWs thus lose their advantages in scattering and absorption mainly because of the following reasons. First, the SiNW cluster after assembly has a diameter that is much larger (several micrometers) than those of individual nanowires (several tens of nanometers). This result implies strong scattering and absorption resulting from the enhancement of the resonant field. This enhancement is due to the diameter being smaller than that of the visible light wavelength. Second, the SiNWs embedded in the cluster are aligned in the same direction and may thus have weak diffuse reflectivity. Finally, SiNWs are covered by CTAB and may decrease absorption.

The detection mechanism of the SiNW colorimetric sensor was first examined through ultraviolet–visible (UV–vis) spectroscopy. The SiNWs were first dispersed in CATA. KF was then introduced, and the UV–vis spectra were collected every 10 min (**Figure 3**A). The results reveal that the system attains the strongest absorption at 415 nm, crossing 380–500 nm. The absorption property matches the yellow color of the system because the system should appear yellow after this band is absorbed from the incoming white light. The most efficient scattering of SiNWs with a diameter of 107 nm is indicated by a yellow color in optical dark-field microscopy according to the scattering efficiency peak at a wavelength of yellow light (around 575 nm).[35] Although the SiNWs used in our experiment have an average diameter of 75 nm (from 50 to 120 nm, Figure 3B), we suppose that the light scattered by SiNWs may also contribute to the yellow appearance after considering the diameter variation as a result of solvation. The UV–vis spectra also reveal that the F^- anion can continuously lower the absorption peaks. Meanwhile, the colors of the system fade and become transparent.

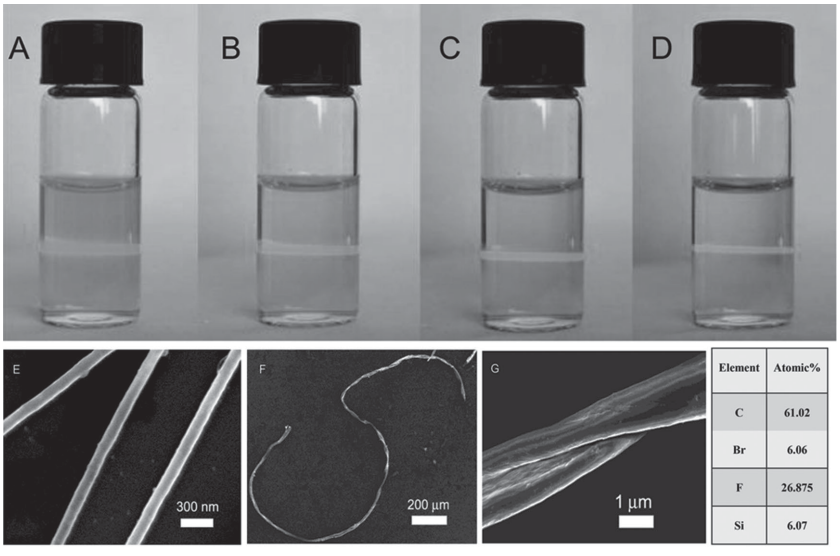

Figure 4. A–D) Tyndall effect on the system every 30 min. E) SEM image of the sample shown in (A). F) SEM image of the sample shown in (D). G) High-resolution SEM image and EDX analysis of (F).

The detection mechanism was investigated further based on the Tyndall effect and scanning electron microscope (SEM) images. The Tyndall effect is also known as Tyndall scattering, which is caused by the scattering of light on particles in a colloid or a fine suspension.[38] The Tyndall effect is widely applied to distinguish suspensions and solutions. **Figure 4**A–D shows the Tyndall scattering of the SiNWs–CTAB–F^- aqueous solution at different times after the introduction of the F^- anion. First, a visible luminous flux can be observed along the path of the incident red laser beam even though the system appears transparent under sunlight (Figure 4D). This result indicates that the color and UV–vis absorption changes are not induced by the elimination of SiNWs from the system (i.e., SiNWs were dissolved by F^-). Second, the Tyndall scattering can be strong enough to cause the pink appearance of the aqueous phase after the introduction of the F^- anion (Figure 4A). However, the scattering subsequently weakens in 90 min until only the main luminous flux can be observed (Figure 4B–D).

The SEM images of the SiNWs at the beginning (Figure 4A) and at 90 min (Figure 4D) are shown in Figure 4E,F, respectively. The SiNWs are well dispersed when the system shows the strongest Tyndall scattering, and they assemble into a helix structure when the system becomes transparent. The helix structure can reach a length of 4 mm, with a maximum diameter of ≈3 μm. Figure 4G shows an enlarged section of Figure 4F and reveals that the assembled helix has a right-handed rotation similar to several other self-assembled helix nanostructures.[39] The EDX spectra of the assembled structure reveal that the structure contains C, Br, Si, and F. These four elements are typically present concurrently although their atomic ratios vary with detection position. The result is in accordance with the self-assembling mechanism illustrated in Figure 2.

The detection limit was also investigated for F^- monitoring application in pure water. The work designed a testing process which satisfies the requirements of 1.2–0.7 ppm F^- in water that is recommended by the US Health and Human Services.[30] It was observed that when the F^- concentration is 1 ppm, the color of the system could still change from yellow to transparent, but this process will take at least 3 h at room temperature. However, we also noted that detection time can be significantly reduced by increasing the temperature. An optimized process shows that it only needs 10 min at 70 °C that UV–vis absorption intensity decreased by 25.4% under 1 ppm KF when the reagents were mixed according to the following sequence: SiNWs, KF, and CTAB solution. It should be noted that this detection time is still shorter than traditional organic colorimetric sensors whose detection times are largely delayed by their hydrophobic nature and the strong solvation of F^-. During our optimized detection process, the color changes can also be identified by the naked eye, thus indicating the development of a colorimetric method for 1 ppm F^- detection in pure water.

Table 1. Summary of the F-detection methods in recent years.

Ref.	Environment	Sensor	Mechanism	Limit [ppm]
Our work	Pure water phase	SiNWs	Specific binding	1
[26]	CH_2Cl_2 + water (v:v,–)	Triarylboranes	Lewis acidic	4
[30]	DMSO + water (v:v, 1:9)	$[Ph_4Sb]^+$	Lewis acidic	0.1
[28]	DMSO	Organic	Hydrogen bond	1.9
[29]	CH_2Cl_2	Organic	Si–O cleavage	1
[27]	Acetonitrile	Organic	Si–O cleavage	4.75
[31]	THF or acetone	Polymer	Si–O cleavage	0.1

The observations also reveal that in a controlled experiment the absorption spectra showed negligible change in the same time period when the positions of F^- anion and CTAB in the sequence were reversed. This mixing-procedure dependence may be attributed to the introduction of the F^- anion to the Si–H–CTAB bond. This process is decelerated in the controlled experiment because of the low F^{-1} concentration. The experiment results indicate that F^- may induce the fading of the color of the H-SiNW suspension, and that the kinetics process is affected by CTAB. The 1 ppm detection limitation in the pure water phase that was obtained in our experiment is among the best F^- detection results achieved even in organic or mixed solutions (**Table 1**). The sensitivity and response of the SiNW colorimetric sensor may be improved by optimizing the detection process.

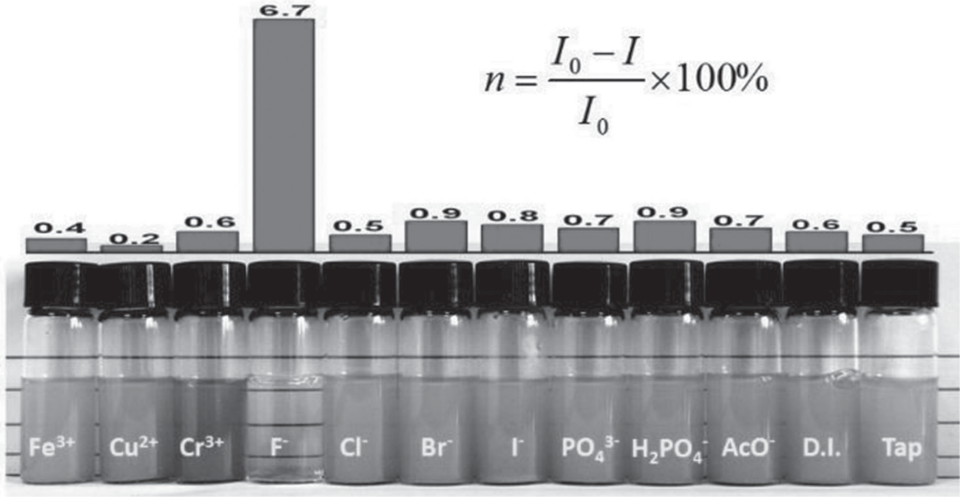

Figure 5. Selectivity of the SiNW colorimetric sensor. The number marked on the histogram is the UV–vis absorption intensity variation at 415 nm after 20 min in room temperature. The value was computed using the formula on the top right, where I_0 and I are the initial absorption intensity and the absorption intensity after 20 min, respectively, at 415 nm. All of the ions have a concentration of 2×10^{-2} mol L^{-1}.

Figure 5 shows the selectivity of the SiNW colorimetric sensor. The concentration of all ions was set as 2×10^{-2} mol L^{-1} to show the strong anti-interference ability. The high F^- detection selectivity of the H-SiNW colorimetric sensor reveals its advantages in the aqueous phase. First, strong fluorescence quenchers such as Cr^{3+} and Cu^{2+} do not interfere with the detection. Second, the color of the SiNW suspension undergoes only a negligible change in the presence of numerous common anions and tap water. Third, the detection results are adequately stable; the SiNW suspensions in all the testing vials maintained their color after stocking in room temperature for several weeks.

3. Conclusions

This work developed a new detection strategy using H-SiNWs as stable colorimetric sensors in the label-free detection of F^- anions in the pure water phase. These colorimetric sensors are capable of significantly simplifying the surface decoration of the ultrasensitive, highly selective, and stable nanostructure sensor. The results indicate that this strategy is simple, cheap, highly sensitive, and selective. It suggests that with structural properties and outstanding stability, 1D nanostructure may provide new opportunities in the design of feasible colorimetric detection systems.

4. Experimental Section

SiNWs were synthesized in large scale by using a high-temperature tube furnace. The temperature in the tube was measured by a movable thermometer. The uniform temperature zone in the 76 cm long furnace was ≈15 cm. An Al_2O_3 boat loaded with 1.00 g SiO powder (Sigma-Aldrich, 325 mesh, 99.9%) was placed in the middle of a 130 cm long alumina tube, and 25.00 g Sn slat loaded onto another Al_2O_3 boat (10 cm long) was placed 16.5 cm (1048 °C) downstream from the SiO source (center to center). The length of the alumina tube is critical to growth because it affects the flying distance and condensing location of SiO vapor. After the system was pumped to 5×10^{-2} mbar, nitrogen was flown in to increase pressure to 350 mbar. The system was heated to 1350 °C at a rate of 50 °C min^{-1}, and then maintained at this temperature for ≈80 min of growth. After natural cooling to room temperature, a yellowish-brown product ≈2 × 8 cm was obtained on the Sn surface across the 600–1200 °C zone. This product was first subjected to SEM (Philips XL30 FEG). Some of the as-prepared or HF (10%, v:v)-treated samples were then dispersed in ethanol. Then, a drop of the dispersion was placed on a carbon-coated copper sample grid for transmission electron microscopy (TEM; Philips CM20, operated at 200 kV). The F^- anion detection and other contrast ions detection were performed by titrating the SiNWs water suspension. The visible light absorption was determined on a UV–vis–NIR spectrophotometer (Varian Cary 5000).

Acknowledgements

The work was partially supported by the National Basic Research Program of China (973 program) (Grant Nos. 2012CB932400 and 2013CB933500), the National Natural Science Foundation of China (Grant Nos. 51172246 and 51373188), the Major Research Plan of the National Natural Science Foundation of China (Grant No. 91233110).

Received: May 20, 2014
Revised: October 6, 2014
Published online: January 22, 2015

[1] H. J. Mamin, M. Kim, M. H. Sherwood, C. T. Rettner, K. Ohno, D. D. Awschalom, D. Rugar, *Science* **2013**, *339*, 557.
[2] G. S. Shekhawat, V. P. Dravid, *Nat. Nanotechnol.* **2013**, *8*, 77.
[3] E. R. Kay, J. Lee, D. G. Nocera, M. G. Bawendi, *Angew. Chem. Int. Ed.* **2013**, *52*, 1165.
[4] X. D. Wang, J. A. Stolwijk, T. Lang, M. Sperber, R. J. Meier, J. Wegener, O. S. Wolfbeis, *J. Am. Chem. Soc.* **2012**, *134*, 17011.
[5] D. Khatayevich, T. Page, C. Gresswell, Y. Hayamizu, W. Grady, M. Sarikaya, *Small* **2014**, *24*, 1505.
[6] T. A. Taton, C. A. Mirkin, R. L. Letsinger, *Science* **2000**, *289*, 1757.
[7] N. L. Rosi, C. A. Mirkin, *Chem. Rev.* **2005**, *105*, 1547.
[8] J. M. Nam, S. I. Stoeva, C. A. Mirkin, *J. Am. Chem. Soc.* **2004**, *126*, 5932.
[9] P. W. Wu, K. Hwang, T. Lan, Y. Lu, *J. Am. Chem. Soc.* **2013**, *135*, 5254.
[10] Y. Cao, R. Jin, C. A. Mirkin, *J. Am. Chem. Soc.* **2001**, *123*, 7961.
[11] L. Latterini, M. Amelia, *Langmuir* **2009**, *25*, 4767.
[12] C. J. Kirubaharan, D. Kalpana, Y. S. Lee, A. R. Kim, D. J. Yoo, K. S. Nahm, G. G. Kumar, *Ind. Eng. Chem. Res.* **2012**, *51*, 7441.
[13] Y. Zhou, S. Wang, K. Zhang, X. Jiang, *Angew. Chem. Int. Ed.* **2008**, *47*, 7454.
[14] J. J. Storhoff, A. D. Lucas, V. Garimella, Y. P. Bao, U. R. Muller, *Nat. Biotechnol.* **2004**, *22*, 883.
[15] S. J. Park, T. A. Taton, C. A. Mirkin, *Science* **2002**, *295*, 1503.
[16] E. Morales-Narváez, A. Merkoçi, *Adv. Mater.* **2012**, *24*, 3298.
[17] Y. Song, K. Qu, C. Zhao, J. Ren, X. Qu, *Adv. Mater.* **2012**, *22*, 2206.
[18] Y. Hu, X. Gao, L. Yu, Y. Wang, J. Ning, S. Xu, X. W. Lou, *Angew. Chem. Int. Ed.* **2013**, *52*, 5636.
[19] J. B. Blanco-Canosa, I. L. Medinta, D. Farrell, H. Mattoussi, P. E. Dawson, *J. Am. Chem. Soc.* **2010**, *132*, 10027.
[20] J. Liu, S. Mendoza, E. Román, M. J. Lynn, R. Xu, A. E. Kaifer, *J. Am. Chem. Soc.* **1999**, *121*, 4304.
[21] I. Tokareva, S. Minko, J. H. Fendler, E. Hutter, *J. Am. Chem. Soc.* **1999**, *126*, 15950.
[22] J. Li, S. Yang, W. Zhou, C. Liu, Y. Jia, J. Zheng, Y. Li, J. Li, R. Yang, *Chem. Commun.* **2013**, *49*, 7932.
[23] T. Zheng, R. Zhang, Q. Zhang, T. Tan, K. Zhang, J. Zhu, H. Wang, *Chem. Commun.* **2013**, *49*, 7881.
[24] Z. Wu, Z. K. Wu, H. Tang, L. J. Tang, J. H. Jiang, *Anal. Chem.* **2013**, *85*, 4376.
[25] R. B. Bakhi, K. Sethupathi, S. Ramaprabhu, *J. Phys. Chem. B* **2009**, *113*, 3190.
[26] C. R. Wade, I. S. Ke, F. P. Gabba, *Angew. Chem. Int. Ed.* **2012**, *51*, 478.
[27] O. A. Bozdemir, F. Sozmen, O. Buyukcakir, R. Guliyev, Y. Cakmak, E. U. Akkaya, *Org. Lett.* **2010**, *12*, 1400.
[28] B. Sui, B. Kim, Y. Zhang, A. Franzer, K. D. Belfield, *ACS Appl. Mater. Interfaces* **2013**, *5*, 2920.
[29] J. Cao, C. Zhao, P. Feng, Y. Zhang, W. Zhu, *RSC Adv.* **2012**, *2*, 418.
[30] I. S. Ke, M. Myahkostupov, F. N. Castellano, F. P. Gabbaï, *J. Am. Chem. Soc.* **2012**, *134*, 15309.
[31] J. M. Hu, G. Y. Zhang, Y. H. Geng, S. Y. Liu, *Macromolecules* **2011**, *44*, 8207.
[32] S. J. Lee, J. M. Baik, M. Moskovits, *Nano Lett.* **2008**, *8*, 3244.
[33] D. D. D. Ma, C. S. Lee, F. C. K. Au, S. T. Lee, *Science* **2003**, *299*, 1874.
[34] R. A. Street, W. S. Wong, C. Paulson, *Nano Lett.* **2009**, *9*, 3494.
[35] G. Brönstrup, N. Jahr, C. Leiterer, A. Csáki, W. Fritzsche, S. Christiansen, *ACS Nano* **2012**, *4*, 7113.
[36] H. Wang, X. H. Zhang, X. M. Meng, S. M. Zhou, S. K. Wu, W. S. Shi, S. T. Lee, *Angew. Chem. Int. Ed.* **2005**, *44*, 6934.
[37] C. C. Wu, M. J. Sailor, *ACS Nano* **2013**, *7*, 3158.
[38] T. C. Ozawa, K. Fukuda, Y. Ebina, T. Sasaki, *Inorg. Chem.* **2013**, *52*, 415.
[39] Q. Zhang, M. Q. Zhao, D. M. Tang, F. Li, J. Q. Huang, B. Liu, W. C. Zhu, Y. H. Zhang, F. Wei, *Angew. Chem. Int. Ed.* **2010**, *49*, 3642.